Structural Studies on Peptides Corresponding to Mutants of the Major α-Helix of Barnase†

Alistair D. Kippen, Vickery L. Arcus, and Alan R. Fersht*

Medical Research Council Unit for Protein Function and Design, Department of Chemistry, University of Cambridge, Lensfield Road, Cambridge, CB2 1EW, U.K.

Received April 22, 1994; Revised Manuscript Received June 20, 1994®

ABSTRACT: The structures of a family of peptides that contain variants of the major α-helix of barnase (residues 6–18) have been analyzed in solution by circular dichroism (CD) and ^{1}H NMR at various concentrations of the helix-inducing cosolvent trifluoroethanol (TFE). The very low equilibrium constant ($\sim 10^{-2}$) for the formation of helix in water, K^{H_2O}, was estimated from titration of the helical ellipticity signal at 222 nm with [TFE] using the equation, $K^{TFE} = K^{H_2O} \exp((m/RT)[TFE]/[H_2O])$, where K^{TFE} is the equilibrium constant for the formation of helix in TFE/H_2O and m is characteristic for each peptide but appears to be proportional to the lengths of related helices. NMR studies show that the peptide is mainly random coil in water, but that the helix is induced cooperatively by TFE and extends from residues 6 to 18 for wild-type peptide in 35% TFE. The mutant peptide Tyr-17→Ala, however, has a helical region extending only for residues 9–15. Truncation of the helix upon mutation is also detected in the TFE titration procedure, which finds correspondingly lowered m-values upon mutation. This is is also supported by measurements of the pH dependence of K^{H_2O}, which is caused by the ionization of the C-cap residue, His-18, whose pK_a is raised by the interaction of the protonated form with the helix dipole. Whereas there is an apparent charge/dipole interaction energy of 1.1 kcal mol^{-1} in the wild-type peptide, similar to that measured in the native protein, this drops dramatically upon mutations that disrupt the C-terminus of the helix. Mutation of Tyr-17→Ala lowers K^{H_2O} only slightly, as do the other helix-destabilizing mutations. The combined results show that the helix-weakening effects of mutations act here primarily by shortening the length of the helix, with smaller effects on the equilibrium constants between helix and coil (K^{H_2O}). Such effects would not be detected by simple measurements on the percentage helicity of peptides measured by the amplitude of the CD signal at 222 nm. TFE appears to act by perturbing a preexisting equilibrium between unfolded and fully helical peptides since NMR studies at TFE concentrations spanning those for the helix–coil transition suggest a predominance of one folded state. This is to be expected since m increases with increasing helical length, and so TFE selectively stabilizes the longest helix. Data acquired in the presence of TFE give information on the longest helices, but there is evidence that shorter ones may exist in the absence of TFE.

The regions of a protein that could initiate its folding may perhaps be detected from the formation of local secondary structure in the unfolded state (Tanford, 1968, 1970; Karplus et al., 1973; Shortle & Meeker, 1986; Dill & Shortle, 1991; Ptitsyn, 1991; Neri et al., 1992). Fragments of a protein may mimic the unfolded state and allow the analysis of local interactions while eliminating the complication of tertiary interactions (Wright et al., 1988; Shortle & Meeker, 1989; Kim & Baldwin, 1990; Dyson & Wright, 1991; Dyson et al., 1992a,b; Sancho & Fersht, 1992; Kuroda, 1993; Shin et al., 1993a,b; Waltho et al., 1993; Kippen et al., 1994). Whereas the detection of structure that is largely formed in peptides is relatively routine by spectroscopy, the presence of small fractions of ordered structure in equilibrium with predominantly random coil conformations is not only difficult to detect but also difficult to define. Does the detection of, for example, 3% helical structure mean that 3% of the population is in a fully helical conformation, or are there regions of fluctuating structure as for "nascent" helices (Wright et al., 1988)?

The detection of α-helices has been aided by the use of trifluoroethanol (TFE), which induces the formation of helical structure in peptides and protein fragments that are mainly or partly unstructured in aqueous solution but have a helical propensity (Goodman et al., 1971; Chen & Sonnenberg, 1977; Bierzynski et al., 1982; Kim et al., 1982; Shoemaker et al., 1985; Nelson & Kallenbach, 1986; 1989; Brems et al., 1987; Dyson et al., 1988; Lehrman et al., 1990; Sönnichsen et al., 1992). The exact mechanism by which TFE stabilizes secondary structure is unknown, but more recent studies suggest that TFE interacts preferentially with the helical conformation of a peptide to shift the structural equilibrium toward this state (Nelson & Kallenbach 1986; Merutka & Stellwagen, 1989; Lehrman et al., 1990; Sönnichsen et al., 1992; Shin et al., 1993a,b; Jasanoff & Fersht, 1994). It has been shown that the stabilization of helical conformations in protein fragments by TFE tends to be restricted to those regions that are helical in the native protein, although this is not always the case (Liu et al., 1994). Therefore, the "stop signals" of α-helices can persist, and helical conformations develop in those regions with a high helical-forming propensity or preexisting helical structure (Gooley & MacKenzie, 1988; Nelson & Kallenbach, 1989; Lehrman et al., 1990; Sönnichsen et al., 1992; Sancho et al., 1992b).

Previously, we attempted to analyze the titration of the formation of helix with quantitatively increasing [TFE] (Sancho et al., 1992b) and have since derived the following equation (eq 1), which describes the titration curves satisfactorily (Jasanoff & Fersht, 1994):

† A.D.K. is suppported by a Medical Research Council studentship award. V.L.A. is supported by a Prince of Wales Scholarship (Cambridge Commonwealth Trust).

* Author to whom all correspondence should be addressed.

® Abstract published in *Advance ACS Abstracts,* August 1, 1994.

0006-2960/94/0433-10013$04.50/0

$$\Delta G^{TFE} = \Delta G^{H_2O} - m[TFE]/[H_2O] \quad (1)$$

where ΔG^{TFE} is the free energy of folding of the peptide in TFE/H_2O mixtures, ΔG^{H_2O} is the free energy in water, and m is a peptide-specific constant that appears to be proportional to the length of the helix for related helices. A useful feature of this equation is that it can be used to calculate the equilibrium constant for the formation of the peptide in the absence of TFE. The equilibrium constant, K^{TFE}, for the formation of peptide is from eq 1: $K^{TFE} = K^{H_2O} \exp((m/RT)[TFE]/[H_2O])$.

The procedure has been applied to two peptides of barnase, the 110 residue extracellular ribonuclease of *Bacillus amyloquefaciens*, that correspond to the sequences 5–21 and 1–36, which contain its first major helix (residues 6–18) and its second helix (26–34). The peptides form 3% and 6% helical structure, respectively, in water at pH 6.3 and 25 °C (Sancho & Fersht, 1992; Sancho et al., 1992a,b; Kippen et al., 1994). This major helix has been predicted to act as a nucleation site, initiating the folding of barnase [J. Moult, personal communication; reported by Serrano et al. (1992)], and is largely formed in the folding intermediate (Matouschek et al., 1990, 1992; Fersht, 1993).

We now investigate the structures of a series of peptides that correspond to sequences containing the major α-helix of barnase and some of its mutants. This is for two reasons. The first is to test the utility of eq 1 by extension to a series of related peptides to determine whether it can detect predictable changes in them. The second is that we have found that the mutations concerned can alter the timing of formation of the major helix in the folding pathway of native barnase (Matouschek & Fersht, 1993; J. Matthews and A. R. Fersht, unpublished). The residues mutated, Thr-16, Tyr-13, and Tyr-17, are buried on the opposite side of the helix from that which packs against the β-sheet (Mauguen et al., 1982; Bycroft et al., 1990; Matouschek et al., 1992), and they make a hydrophobic patch whereby the side chain of Tyr-13 packs against that of Tyr-17 which packs against the γ-methyl of Thr-16. The sequence of the peptide designated (1–22) is A(1)Q(2)V(3)I(4)N(5)T(6)F(7)D(8)G(9)V(10)A(11)D(12)Y(13)L(14)Q(15)T(16)Y(17)H(18)K(19)L(20)P(21)D(22).

The studies using eq 1 and monitoring helix formation by circular dichroism are complemented by an analysis of the structures of peptides (5–21) of barnase directly using ^1H NMR spectroscopy, which has been widely used to define the structures of short peptides (Gooley & MacKenzie, 1988; Wright et al., 1988; Dyson et al., 1992a,b; Sönnichsen et al., 1992; Sancho et al., 1992a,b; Shin et al., 1993a,b; Waltho et al., 1993).

EXPERIMENTAL PROCEDURES

Materials. 2,2,2-Trifluoroethanol (TFE) and cyanogen bromide were from Fluka. Deuterated HCl (^{2}HCl) and NaOH (NaO^{2}H) were from Sigma. Deuterated H_2O (^2H_2O) was from Fluorochem, and deuterated TFE (TFE-d_3) was from MSD Isotopes. The barnase peptide (5–21) was obtained from Calbiochem-Novabiochem (Nottingham, U.K.). All other reagents were of analytical grade and were purchased from either Sigma, Fluka, or Amersham.

Preparation and Purification of Peptides. Peptide 1–22 of barnase and mutants of this peptide [1–22, with the substitution Tyr-17→Ala, 1–22 Y13A, 1–22 Y13&17A, 1–22 T16S, 1–22 H18G, and 5–21 Y17A] were prepared using a peptide synthesizer (Applied Biosystems 432A, Synergy). Each peptide is amide protected at the C-terminal. The peptides were purified by gel filtration using a Sephadex G-15 column (2.1 × 29.8 cm) equilibrated in water at room temperature under a minimum flow by gravity (approximately 1 mL/min) and by preparative reverse-phase HPLC (Dynamax C8 300 Å, 10 × 250 mm column) with a linear gradient of acetonitrile (16–34% in 39 min) in 0.05% trifluoroacetic acid in water.

The identity of each peptide was confirmed by electrospray mass spectrometry (Dr. J. Staunton, Department of Chemistry, Cambridge University), and each was shown to be >99% pure by reverse-phase HPLC. The concentration of tyrosine-containing peptides was determined from the absorbance at 280 nm using a known molar extinction coefficient from model compounds (Gill & von Hippel, 1989). The concentration of peptide (1–22 Y13&17A) was determined from the dry weight of the peptide and by protein assay using the method of Bradford (1976).

The buffers used were as follows: 5 mM MES (i) pH 5.3, prepared from dilution of a 50 mM stock solution containing 43 mM acid form and 7 mM sodium salt; (ii) pH 5.8, prepared from dilution of a 50 mM stock solution containing 32 mM acid form and 18 mM sodium salt; (iii) pH 6.3, prepared from dilution of a 50 mM stock solution containing 18 mM acid form and 32 mM sodium salt; (iv) pH 6.7, prepared from dilution of a 50 mM stock solution containing 9 mM acid form and 41 mM sodium salt; (v) pH 7.0, prepared from dilution of a 50 mM stock solution containing 5 mM acid form and 45 mM sodium salt; and 5 mM MOPS (vi) pH 7.3, prepared from dilution of a 50 mM stock solution containing 19 mM acid form and 31 mM sodium salt; (vii) pH 7.8, prepared from dilution of a 50 mM stock solution containing 8 mM acid form and 42 mM sodium salt.

Peptide solutions were immediately stored at −72 °C following dissolution, and fresh aliquots were employed because Yoshida et al. (1993) found that the barnase peptide 1–24, which has predominantly random coil structure as a monomer, polymerizes after a lag period of approximately 5 days upon incubation at a concentration of 0.2 mM at 5 °C, forming helical structure.

Trifluoroethanol Titrations. CD spectra (far-UV) of peptide 1–22 at a concentration of 3 μM were recorded in a series of TFE (0–37%) solutions in buffer at 25 °C using a JASCO J-720 spectropolarimeter. Titrations were recorded in the series of different buffers, pH 5.3–7.0 5 mM MES and pH 7.3 and 7.8 5 mM MOPS, described above. Data at a range of wavelengths at each pH were analyzed using eq 1 to determine ΔG^{H_2O}, the standard free energy of the equilibrium between folded and unfolded states in water, at each pH. From the dependence of ΔG^{H_2O} on pH, the pK_a of histidine 18 in both the unfolded and folded conformations of the peptide was determined using eq 3 (see Results). ΔG^{H_2O} values of each mutant peptide [1–22 Y17A, 1–22 Y13A, 1–22 Y13&17A, 1–22 T16S, and 1–22 H18G (control)] at a series of pH values 5.3–7.8 were also determined from a similar procedure to in turn determine the pK_a of His-18 in the unfolded and folded conformations of each peptide.

TFE titrations of peptide 1–22 at concentrations of 1, 6, and 15 μM were recorded in pH 5.8 buffer at 25 °C to determine ΔG^{H_2O} at each peptide concentration. TFE titrations of peptide 1–22 at a concentration of 3 μM were recorded in (i) pH 5.8 buffer at 25 °C in 0.5 and 1 M KCl, (ii) pH 6.7 buffer at 25 °C in 1 M KCl, and (iii) pH 7.3 buffer at 25 °C in 1 M KCl to determine ΔG^{H_2O} at each salt concentration at each pH. The CD signal of peptide 1–22 at a concentration

of 3 μM in pH 7 buffer was recorded at 200 nm from 1 to 60 °C in both H_2O and 37% TFE.

^1H NMR Spectra of Peptides in H_2O and TFE. Samples were prepared by dissolving lyophilized peptide 5–21 in (i) 90% H_2O/10% ^2H_2O; (ii) 80% H_2O/10% ^2H_2O/10% TFE-d_3; (iii) 75% H_2O/10% ^2H_2O/15% TFE-d_3; and (iv) 55% H_2O/10% ^2H_2O/35% TFE-d_3 solutions. Lyophilized peptide 5–21 Y17A was dissolved in a solution of 55% H_2O/10% ^2H_2O/35% TFE-d_3. The pH was adjusted by using small aliquots of 0.25 M NaO^2H or ^2HCl solutions, and pH values in $^2H_2O/H_2O$ solutions refer to uncorrected meter readings. All spectra were recorded at pH 4.5 ± 0.05 at 6 °C using a Bruker AMX500 spectrometer equipped with an X32 computer. Final peptide concentrations were 2.0–2.3 mM. Chemical shifts were referenced to the internal standard 3-(trimethylsilyl)propionic acid-*2,2,3,3-d_4* sodium salt (TSP). All 2-dimensional spectra were recorded in the phase sensitive mode using time proportional phase incrementation (Redfield & Kunz, 1975; Marion & Wüthrich, 1983). Double quantum filtered correlation spectroscopy (DQF-COSY) (Piantini et al., 1982) and total correlation spectroscopy (TOCSY) (Bax & Davis, 1985) were used for spin system assignments. Nuclear Overhauser effect spectroscopy (NOESY) (Jenner et al., 1979; Kumar et al., 1980) was also used to complete sequence specific assignments and investigate the structure of the peptide. Several NOESY spectra were recorded for each sample over a range of mixing times (100–600 ms). For all spectra, suppression of the water signal was achieved by presaturation. Generally, spectra were recorded with 2048 data points in t_2 and 400–512 t_1 increments, and 32–128 transients per increment were collected. Data processing was carried out using the Bruker UXNMR software package. Spectra were Fourier transformed in both ω_2 and ω_1 using $\pi/3$ and $\pi/5$ phase-shifted sine-bell window functions, respectively; the final matrices contained 2048 × 1024 real data points in ω_2 and ω_1.

Sequence Specific Resonance Assignments. Proton spin system assignments were made from the DQF-COSY spectra, and these were confirmed by reference to the TOCSY spectra. $C^\delta H$ and $C^\epsilon H$ proton assignments for the aromatic residues Phe-7, Tyr-13, and Tyr-17 were demarcated by the presence of a strong intraresidue NOE between the $C^\beta H$ and $C^\delta H$ protons. Sequence specific assignment (Wüthrich, 1986) of the peptide 5–21 in 90% H_2O/10% ^2H_2O and 80% H_2O/10% ^2H_2O/10% TFE-d_3 solutions followed directly from the presence of characteristic interresidue $C^\alpha H$, NH(i, i + 1) NOEs (Wright et al., 1988). For Pro-21, a medium strength NOE from the Leu-20 $C^\alpha H$ to the Pro-21 $C^\delta H$ resonance is seen for the *trans* isomer, which is characteristic for proline residues in extended chain conformations. Many more short and medium range NOEs were seen for the peptide 5–21 in 35% and 15% TFE solutions, as compared with those in water and 10% TFE, and assignments for the peptide 5–21 in 35% and 15% TFE solutions were made by standard procedures (Wüthrich, 1986).

RESULTS

Selection of Peptides. The peptide (1–22) contains only the N-terminal α-helix of barnase, which allows specific study of this particular element of secondary structure. The peptide 5–21 was chosen for ^1H NMR studies since the first four residues of barnase are disordered in the native structure (Mauguen et al., 1982; Bycroft et al., 1990). The behavior of 1–22 and 5–21 is, in general, very similar (Kippen et al., 1994). The chosen mutations in peptide 1–22 were of those residues that make the highly stabilizing interactions within the native α-helix: Tyr-13, Thr-16, and Tyr-17 (Mauguen et al., 1982; Bycroft et al., 1990; Serrano et al., 1992; J. Matthews & A. R. Fersht, unpublished; A. Buckle, personal communication).

Trifluoroethanol Titrations. CD spectra of the peptide 1–22 in water (see Figure 1) suggest that it adopts a random coil conformation in water. The CD spectra become more helix-like with increasing concentrations of TFE, showing the development of a small shoulder at 222 nm and a minimum at 208 nm. The shoulder at 222 nm in spectra of the wild-type peptide is very weak due to the contribution of a positive CD band in this region from Tyr-13 to Tyr-17, which partly neutralizes the signal from the α-helix (Chakrabartty et al., 1993; Vuilleumier et al., 1993). The shoulder at 222 nm is much stronger in the spectra of peptides with the tyrosines mutated. The equilibrium between folded and unfolded conformations of each peptide was analyzed using eq 1. The molar ellipticity of each peptide as a function of the concentration of TFE, at a series of wavelengths and at each pH, was fit to an expression derived from eq 1 (see Figure 2):

$$\Theta = \Theta_{TFE} + \Theta_{H_2O} \exp(1/RT(m[TFE]/[H_2O] - \Delta G^{H_2O}))/ (1 + \exp(1/RT(m[TFE]/[H_2O] - \Delta G^{H_2O}))) \quad (2)$$

where Θ_{TFE} is the ellipticity in maximal TFE concentration, Θ_{H_2O} is the ellipticity in water, and [TFE]/[H_2O] is the mole ratio of TFE to H_2O. [TFE]/[H_2O] = 0.25(%TFE/(100 − %TFE)) (the %TFE = vol/vol % of TFE).

ΔG^{H_2O} was found to be independent of peptide and salt concentrations within the experimental conditions. There is an isodichroic point in each titration at 203 nm, which is a good indication that the coil to helix transition is a two-state process and that all structure-forming residues in the peptide act in concert (Woody, 1985; Merutka & Stellwagen, 1987, 1991). The isodichroic point remains at a constant wavelength with each mutant of the peptide 1–22. The results are not obscured by aggregation of the peptides, since the CD signal was not dependent on the peptide concentration within experimental conditions. Increasing the temperature from 1 to 60 °C results in a non-cooperative transition in the CD signal of the peptide in water and TFE at 200 nm (data not shown). This is in agreement with the work of Merutka and Stellwagen (1989) and Sönnichsen et al. (1992), which indicates that small peptides may form a more ordered structure at lower temperature, although this effect becomes negligible as the length of the peptide increases. Data are summarized in Table 1.

pH Dependence of ΔG^{H_2O}. ΔG^{H_2O} was found to vary with pH for the wild-type peptides and all of the mutants bar His-18→Gly. There are two possible reasons for this: firstly, that there is a pH-dependent contribution of His-18 to the CD signal at 222 nm, or secondly, that the pH dependence results from the ionization of His-18. We favor the latter explanation since studies on native barnase have shown that His-18 contributes very little to its CD spectrum within this pH range (Vuilleumier et al., 1993) and that the stability of barnase is influenced by the ionization of His-18 (Sali et al., 1988; Loewenthal et al., 1991). The protonated form of the histidine acts favorably with the dipole of the helix. The dependence of ΔG^{H_2O} on pH fits excellently to the theoretical equation of a single ionization (Fersht, 1985):

$$K^{H_2O} = (K_a^{coil} K^{H_2O} + [H^+] K^{H_2O}{}_{His^+})/(K_a^{coil} + [H^+]) \quad (3)$$

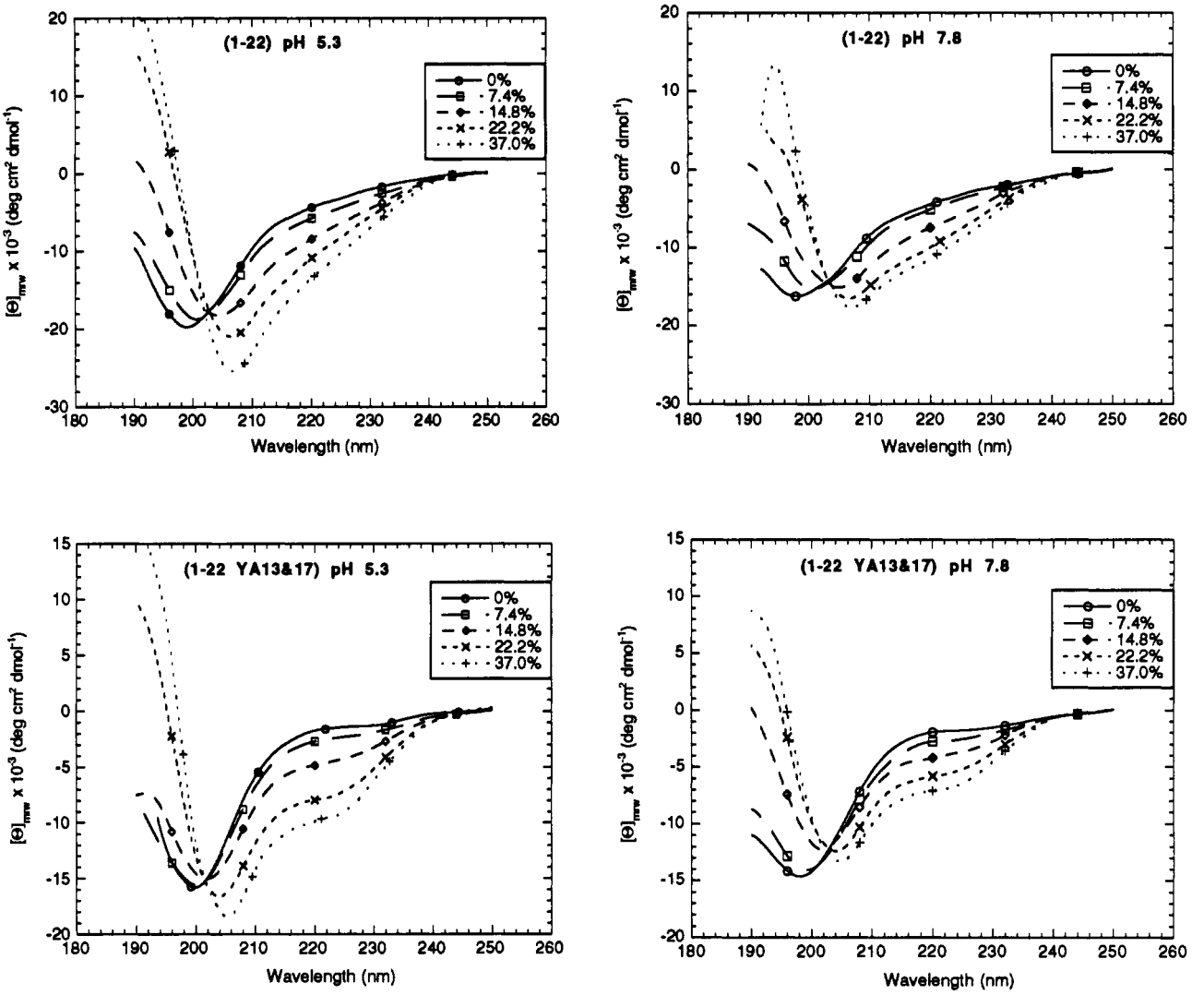

FIGURE 1: TFE titrations of the peptides 1–22 and 1–22 Y13&17A in 5 mM MES (pH 5.3) and 5 mM MOPS (pH 7.8). The CD spectra (far-UV) of each peptide in a concentration of 3 μM were recorded in a series of 11 TFE solutions (0–37%) at 25 °C.

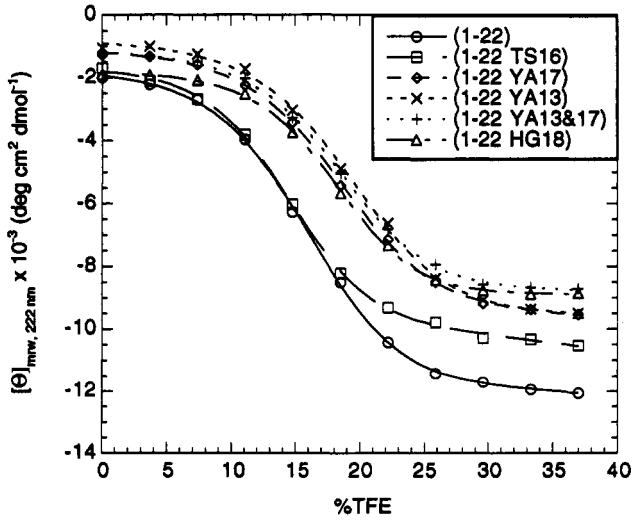

FIGURE 2: Titration of Θ_{222} with [TFE] for each peptide in 5 mM MES (pH 6.3) at 25 °C, fitting data to eq 2 (see text).

(see Figure 3) where K^{H_2O} is the observed equilibrium constant between the folded and unfolded conformations of the peptide, K_a^{coil} is the acid dissociation constant (of His-18) in the unfolded state, $K^{H_2O}_{His}$ is the equilibrium constant for the peptide at high pH (when His-18 is unprotonated), and $K^{H_2O}_{His^+}$ is the equilibrium constant of the peptide at low pH (when His-18 is protonated). The pK_a of His-18 in the unfolded conformation of each peptide, pK_a^{coil}, was determined (see Table 2) and found to be remarkably constant at 6.54–6.56, which is close to the value of 6.52 ± 0.03 found for His-18 in denatured barnase (Loewenthal et al., 1992).

The pK_a of His-18 in the folded conformation of each peptide was calculated from a thermodynamic cycle: $pK_a^{helix} = pK_a^{coil} + \log(K^{H_2O}_{His^+}/K^{H_2O}_{His})$. It is highest for the wild-type peptides. The wild-type peptides 1–22 and 5–21 have very similar values of pK_a^{helix}, pK_a^{coil}, $K^{H_2O}_{His}$, and $K^{H_2O}_{His^+}$ (see Table 2).

pH Dependence of $\Delta\Theta_{222}$. The change in ellipticity at 222 nm ($\Delta\Theta_{222}$) appears to titrate with pH (see Table 1), largely due to the dependence of Θ_{222}^{TFE}, the ellipticity of the folded peptide, on pH. This is most noticeable for the wild-type peptide. As there is little change in the spectra of the mutant His-18→Gly with pH, this titration is a result of helix stabilization at low pH upon protonation of His-18.

^{1}H NMR Studies on the Structure of Peptides. (i) Structure of 5–21 in Water. The presence of strong and medium strength NOEs between α and N(i, i + 1), or in the case of proline 21, between Lys-20 C$^\alpha$H and Pro-21 C$^\delta$H, are indicative of extended chain conformations. However, deviations in chemical shift from random coil values are seen for many residues (see Table 3) and, in conjunction with the presence of weak N,N(i, i + 1) and β,N(i, i + 1) NOEs (see Figures 4A and

Table 1: TFE Titration Data for Peptides 1–22[a]

peptide 1–22	pH	ΔG^{H_2O} [b] (kcal mol^{-1})	$1/K^{H_2O}$ ([coil]/[helix])	m (kcal mol^{-1})	Θ_{222}^{TFE} ($\times 10^{-3}$) (deg cm^2 dmol^{-1})	$\Theta_{222}^{H_2O}$ ($\times 10^{-3}$) (deg cm^2 dmol^{-1})	$\lvert\Delta\Theta_{222}\rvert$ ($\times 10^{-3}$) (deg cm^2 dmol^{-1})
wt	5.3	1.96 ± 0.12	27 ± 6	38 ± 2	−14 ± 1	−1.9 ± 0.2	12 ± 1
	5.8	2.01 ± 0.09	30 ± 5	40 ± 4	−13 ± 1	−1.0 ± 0.1	12 ± 1
	6.3	2.14 ± 0.14	37 ± 9	36 ± 4	−13 ± 2	−1.6 ± 0.2	11 ± 2
	6.7	2.33 ± 0.13	51 ± 13	40 ± 3	−11 ± 1	−1.1 ± 0.2	10 ± 1
	7.0	2.51 ± 0.14	69 ± 19	40 ± 4	−8.8 ± 0.6	−1.6 ± 0.2	7.2 ± 0.6
	7.3	2.67 ± 0.14	91 ± 24	36 ± 3	−8.7 ± 0.6	−1.8 ± 0.5	6.9 ± 0.8
	7.8	2.85 ± 0.11	123 ± 25	35 ± 3	−8.9 ± 0.9	−1.8 ± 0.6	7.1 ± 1.1
T16S	5.3	2.09 ± 0.07	34 ± 4	29 ± 4	−12 ± 1	−1.8 ± 0.4	10 ± 1
	5.8	2.14 ± 0.10	37 ± 7	31 ± 4	−12 ± 2	−1.7 ± 0.3	10 ± 1
	6.3	2.22 ± 0.07	43 ± 5	33 ± 3	−10 ± 1	−1.3 ± 0.4	8.8 ± 0.9
	7.0	2.54 ± 0.05	73 ± 7	33 ± 3	−8.1 ± 0.3	−1.9 ± 0.2	6.2 ± 0.3
	7.8	2.70 ± 0.10	96 ± 17	33 ± 4	−7.8 ± 0.7	−1.5 ± 0.2	6.3 ± 0.7
Y17A	5.3	2.24 ± 0.11	44 ± 9	29 ± 3	−11 ± 1	−2.0 ± 0.2	9.4 ± 1.2
	5.8	2.27 ± 0.10	46 ± 9	31 ± 3	−11 ± 1	−1.3 ± 0.2	9.6 ± 1.0
	6.3	2.35 ± 0.12	53 ± 12	27 ± 3	−9.6 ± 0.9	−1.2 ± 0.1	8.5 ± 0.9
	6.7	2.46 ± 0.15	64 ± 18	32 ± 5	−8.1 ± 0.8	−1.0 ± 0.2	7.1 ± 0.8
	7.0	2.54 ± 0.15	73 ± 21	33 ± 4	−6.9 ± 0.8	−0.4 ± 0.1	6.5 ± 0.8
	7.8	2.66 ± 0.14	89 ± 23	28 ± 4	−6.6 ± 0.5	−0.7 ± 0.1	5.9 ± 0.5
Y13A	5.3	2.27 ± 0.09	46 ± 8	32 ± 2	−11 ± 1	−1.9 ± 0.2	9.2 ± 1.3
	5.8	2.31 ± 0.08	50 ± 7	27 ± 2	−11 ± 1	−1.9 ± 0.1	8.8 ± 1.2
	6.3	2.37 ± 0.14	55 ± 14	33 ± 3	−9.6 ± 1.1	−1.2 ± 0.1	8.4 ± 1.1
	7.0	2.54 ± 0.15	73 ± 21	30 ± 4	−7.0 ± 0.8	−1.0 ± 0.1	6.0 ± 0.8
	7.8	2.64 ± 0.14	86 ± 24	29 ± 4	−6.6 ± 0.4	−1.0 ± 0.1	5.6 ± 0.4
Y13&17A	5.3	2.40 ± 0.09	58 ± 10	26 ± 2	−11 ± 1	−2.1 ± 0.1	8.9 ± 0.6
	5.8	2.42 ± 0.07	60 ± 8	22 ± 2	−11 ± 1	−1.9 ± 0.2	8.8 ± 0.9
	6.3	2.48 ± 0.07	66 ± 8	26 ± 2	−9.6 ± 0.9	−1.8 ± 0.1	7.7 ± 0.9
	7.0	2.55 ± 0.11	74 ± 15	26 ± 3	−7.1 ± 0.5	−1.6 ± 0.1	5.5 ± 0.5
	7.8	2.63 ± 0.07	85 ± 11	22 ± 2	−6.5 ± 0.7	−1.0 ± 0.1	5.5 ± 0.7
H18G	5.3	2.73 ± 0.09	101 ± 17	37 ± 3	−9.8 ± 1.1	−2.3 ± 0.3	7.6 ± 1.2
	6.3	2.77 ± 0.12	108 ± 24	35 ± 4	−8.7 ± 1.1	−1.9 ± 0.4	6.8 ± 1.2
	7.8	2.78 ± 0.08	110 ± 17	34 ± 2	−8.6 ± 0.9	−1.7 ± 0.2	6.9 ± 0.9

[a] In 5 mM MES buffer (pH 5.3–7) and 5 mM MOPS buffer (pH 7.3, 7.8) at 25 °C. Errors quoted are standard errors of the mean. [b] ΔG^{H_2O} determined from eq 2 (see text).

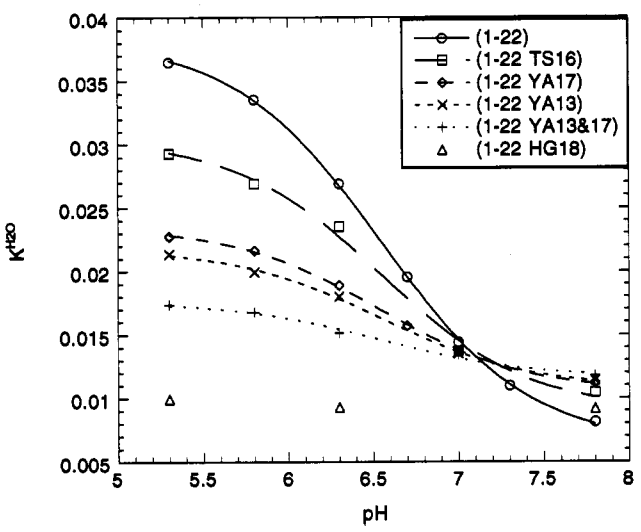

FIGURE 3: Determination of the pK_a of His-18 in each peptide 1–22 from the effect of pH upon ΔG^{H_2O} determined from TFE titrations and eq 3 (see text).

5B), suggest that some turn or helical conformations may be populated.

(ii) Structure of 5–21 in 10% TFE. The presence of medium and strong α,N(i, i + 1) NOEs along the length of the peptide implies that the dominant populations of this peptide in solution are extended strand conformations (see Figure 4B). However, the presence of two weak medium range NOEs, in conjunction with N,N(i, i + 1) NOEs, suggests that structured conformations are populated to a small extent.

(iii) Structure of 5–21 in 15% TFE. Here, there is evidence for populations of near-native barnase structure, including the α-helix (Phe-7-Tyr-17) and the tight turn (Lys-19-Pro-21) (see Figure 4C). The presence of native (i, i + 3) NOE connectivities and one (i, i + 4) NOE peak indicates that a helical conformation encompasses residues 7–17 (see Figure 5A). In addition, there is one non-native (i, i + 3) NOE from Thr-16 to Lys-19, suggesting a conformation where the helix possibly extends outside the region seen in wild-type barnase. All of the medium range NOEs for Lys-19 in the native protein are seen for this peptide, including connectivities to Leu-14 and Tyr-17. This provides good evidence for a native-like tight turn at the C-terminal end of the helix. Strong α, N(i, i + 1) NOEs at the termini (Asp-5-Thr-6-Phe-7 and Tyr-17-His-18-Lys-19) indicate populations of extended strands in these regions.

(iv) Structure of 5–21 in 35% TFE. There is strong evidence that the peptide forms near-native structures under these conditions, where the helix extends from Phe-7 to His-18 and is constrained by a tight turn involving residues Lys-19, Leu-20, and Pro-21 (see Figure 4D). The majority of the medium range (i, i + 3) and (i, i + 4) NOE connectivities found in wild-type barnase for the helical region are seen in this peptide. A native-like structure is also supported by the side chain–side chain NOEs between Tyr-13, Thr-16, and Tyr-17. In addition, the chemical shift for the $^{\gamma}CH_3$ of Thr-16 is pushed upfield from the random coil value to 0.42 ppm by its interaction with the phenolic ring of Tyr-17. Evidence for a native-like tight turn at the end of the helix is provided by the presence of NOEs from Lys-19 to both Tyr-13 and Leu-14.

(v) Structure of 5–21 Y17A in 35% TFE. The mutation of Tyr-17→Ala completely disrupts the near-native structure seen for the wild-type peptide 5–21 under the same conditions (see Figure 4E). No medium range (i, i + 3) connectivities are observed in the region Glu-15–His-18, and only sequential N,N(i, i + 1) connectivities are seen between Thr-6 and Tyr-

Table 2: Limiting Values of K^{H_2O} and Values of pK_a of His-18 Determined from the pH Dependence of TFE Titrations[a]

peptide	$1/K^{H_2O}_{His}$	$1/K^{H_2O}_{HisH^+}$	pK_a^{coil}(His-18)[b]	pK_a^{helix}(His-18)[c]	$\Delta\Delta H^{His-18}_{helix-coil}$[d] (kcal mol^{-1})
1–22	160 ± 4	26.1 ± 0.3	6.55 ± 0.02	7.34 ± 0.03	1.08 ± 0.05
1–22 T16S	112 ± 9	32.8 ± 1.0	6.55 ± 0.03	7.08 ● 0.04	0.72 ± 0.07
1–22 Y17A	95.9 ± 1.5	42.4 ± 0.5	6.54 ● 0.03	6.89 ± 0.05	0.48 ± 0.08
1–22 Y13A	93.0 ± 2.3	45.8 ± 0.8	6.54 ± 0.04	6.85 ± 0.05	0.42 ± 0.09
1–22 Y13&17A	86.2 ± 2.7	56.7 ± 1.1	6.54 ± 0.07	6.72 ± 0.09	0.25 ± 0.14
1–22 H18G	*e*	*e*	*e*	*e*	*e*
5–21[f]	166 ± 7	22.0 ± 0.3	6.56 ± 0.03	7.42 ± 0.04	1.17 ± 0.07

[a] In 5 mM MES buffer (pH 5.3–7) and 5 mM MOPS buffer (pH 7.3, 7.8) at 25 °C, calculated from eq 3. Errors quoted are standard errors of the mean. [b] pK_a of His-18 in the unfolded fragment. [c] pK_a of His-18 in the folded fragment. [d] Difference in interaction energy between His-18 (H^+-form) in helical and unfolded peptide = difference in free energy of folding between high and low pH in water, calculated by $\Delta\Delta G^{His-18}_{helix-coil} = 1.363(pK_a^{helix} - pK_a^{coil})$. [e] Date not determined for control peptide where His-18 is mutated since there is no pH dependence. [f] Data determined for the shorter peptide 5–21 as described for 1–22 (see text).

Table 3: ^{1}H Chemical Shifts of wt Peptide 5–21 in Water at 6 °C, pH 4.5[a]

amino acid	chemical shift (ppm)						
	NH	αH	βH	γH	δH	εH	ζH
Asn-5	8.54	4.72	2.70		7.72, 7.02		
Thr-6	8.27	4.28	4.17	1.13 (Me)			
Phe-7	8.42	4.62	3.13, 3.03		7.23	7.33	7.29
Asp-8	8.38	4.56	2.66				
Gly-9	8.00	3.89					
Val-10	8.05	4.05	2.09	0.93 (Me), 0.95 (Me)			
Ala-11	8.51	4.23	1.32 (Me)				
Asp-12	8.37	4.50	2.68				
Tyr-13	8.16	4.42	3.08		7.11	6.75	
Leu-14	8.13	4.21	1.38, 1.67	1.54	0.83 (Me), 0.89 (Me)		
Gln-15	8.16	4.23	2.02, 2.11	2.35		7.62, 6.97	
Thr-16	8.03	4.16	4.06	1.03 (Me)			
Tyr-17	8.25	4.44	2.88		6.98	6.74	
His-18	8.25	4.54	3.05, 3.18		7.19	8.56	
Lys-19	8.32	4.22	1.73, 1.78	1.43	1.69	3.02	
Leu-20	8.52	4.58	1.63, 1.72	1.66	0.93 (Me), 0.97 (Me)		
Pro-21		4.20	2.14	1.98, 1.94 (t), 1.89 (c)	3.65, 3.77 (t), 3.44, 3.61 (c)		

[a] Chemical shifts that deviate from random coil values by more than 0.1 ppm for nonlabile protons and by more than 0.3 ppm for labile protons are underlined.

13. Here, only a truncated helix appears to be stabilized by TFE.

Analysis of Chemical Shifts (Table 3). The proton chemical shifts for the peptide 5–21 in water (pH 4.5) at 6 °C, which deviate from random coil values by more than 0.3 ppm for amide resonances and by more than 0.1 ppm for nonlabile protons (Wüthrich, 1986), are underlined in Table 3. It is interesting to note that 12 of the 17 C$^\alpha$H resonances do not coincide with random coil values, and this strongly suggests that the backbone of the peptide is sampling structured conformations. In addition, other nonrandom coil chemical shifts are found clustered in the region Tyr-13–His-18. In native barnase, the aromatic rings of Tyr-13 and Tyr-17 pack against each other and also interact with Thr-16, pushing the resonance of the $^\gamma$CH$_3$ of Thr-16 to high field. A similar structural motif populated to a small extent by the peptide would account for the deviations in chemical shift for the Thr-16 (C$^\alpha$H, C$^\beta$H, and $^\gamma$CH$_3$), Tyr-13 (C$^\epsilon$H), Tyr-17 (C$^\delta$H, C$^\epsilon$H), and Leu-14 (C$^\alpha$H, C$^\beta$H) resonances. The resonances that deviate from random coil values are more pronounced for Thr-16 in 5–21 in water than those for Thr-16 in the peptide 1–36 (Sancho et al., 1992b).

For systems in fast exchange, the chemical shift of a given proton is a population-weighted average of the shifts for the same proton in all of the stable conformations adopted by the peptide. If we assume that the populations for 5–21 in aqueous TFE solutions are dominated by either random coil or near-native conformations, then changes in the chemical shift with changing TFE concentration may be used as a qualitative probe in assessing the relative populations of these two states. For example, the chemical shift in the $^\gamma$CH$_3$ resonance of Thr-16 moves incrementally toward its native chemical shift with increasing TFE concentration, reflecting an increase in the population of native-like conformations. This trend is also seen for Ala-11, Tyr-13, Gln-15, Thr-16, and Lys-19 C$^\alpha$H resonances and Asp-12, Leu-14, Thr-16, and Lys-19 NH resonances (see Figure 6). Helix formation in the peptide may be restrained due to the absence of the stabilizing interactions that are formed with the β-sheet in the native protein. Incremental steps in chemical shifts toward the native helical values along the length of the peptide are consistent with an increasing population of the near-native conformation in a pseudo-two-state equilibrium and are inconsistent with, say, a gradual lengthening of the helix with increasing [TFE].

Ninety-five medium range interresidue NOE's define the structure of native barnase in the region Thr-6-Pro-21 (Bycroft et al., 1990). Of these 95 connectivities, 52 are seen for 5–21 in 15% TFE and 51 are seen in 35% TFE. In both cases, these native NOEs are spread along the length of the peptide and indicate that a native-like conformation is populated. It is noted that a significant number of the native NOEs cannot be seen for 5–21 due to spectral overlap. Evidence from chemical shift and NOE data thus indicates that the peptide 5–21 forms a near-native conformation in 35% TFE, which spans the same region that is helical in native barnase (residues 6–18), becoming less populated as the TFE concentration decreases. The peptide forms a longer helix than is indicated by the CD spectra of the peptide at high TFE concentrations under the same conditions. This is mainly due to the presence

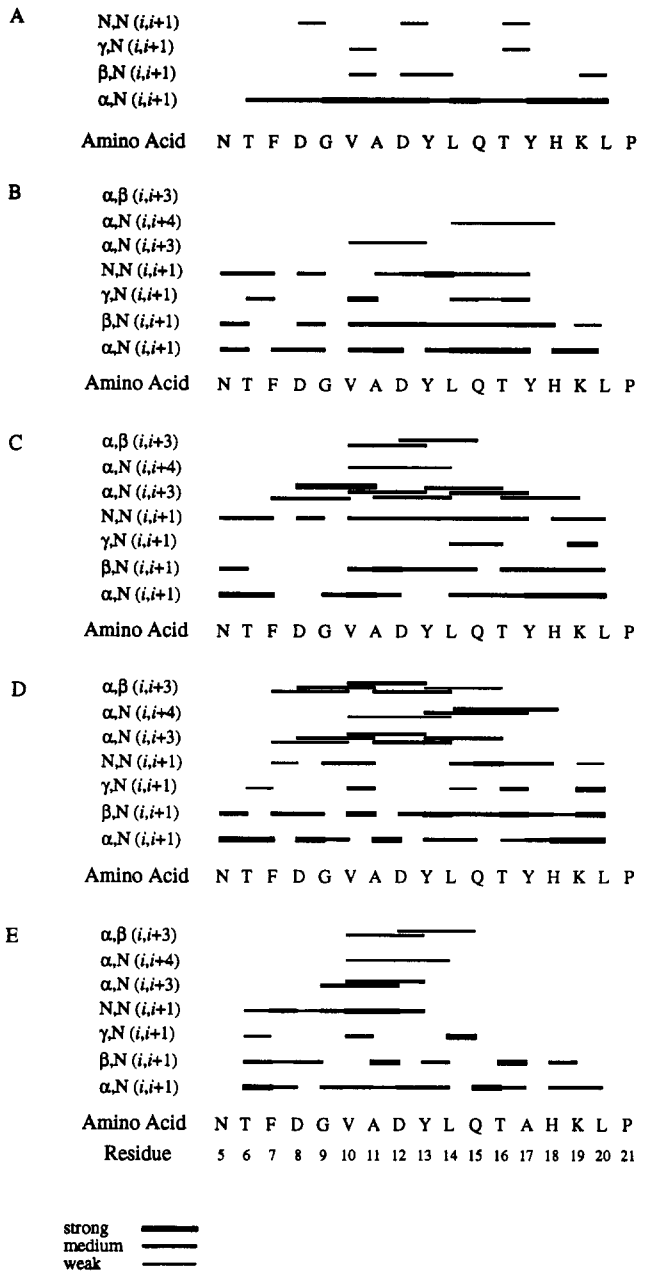

FIGURE 4: Schematic diagram of NOE intensities. NOESY experiments were performed at pH 4.5, 6 °C. Peptide 5–21 in (A) 90% H_2O/10% ^2H_2O, (B) 80% H_2O/10% ^2H_2O/10% TFE-d_3, (C) 75% H_2O/10% ^2H_2O/15% TFE-d_3, and (D) 55% H_2O/10% ^2H_2O/35% TFE-d_3. Peptide 5–21 Y17A in (E) 55% H_2O/10% ^2H_2O/35% TFE-d_3.

of tyrosine residues in the peptide that neutralize some of the CD signal (Chakrabartty et al., 1993), as discussed earlier. Importantly, the NMR data provide strong evidence to suggest that the conformations adopted by the peptide in water and TFE are dominated by random coil and near-native structures. It is the position of this pseudo-two-state equilibrium that is affected by differing concentrations of TFE, rather than the number of residues in the helix-forming region, which remains essentially constant.

NOE connectivities for the peptide 5–21 Y17A in 35% TFE (pH 4.5) at 6 °C indicate that the mutation of Tyr-17 at the C-terminal end of the helix completely disrupts the final turn of the helix (see Figure 4E). In comparison with the wild-type peptide 5–21 in 35% TFE (see Figure 4D), all medium range and N,N(i, i + 1) connectivities are lost from Glu-15 to Pro-21. However, the helix is still formed from Gly-9 to

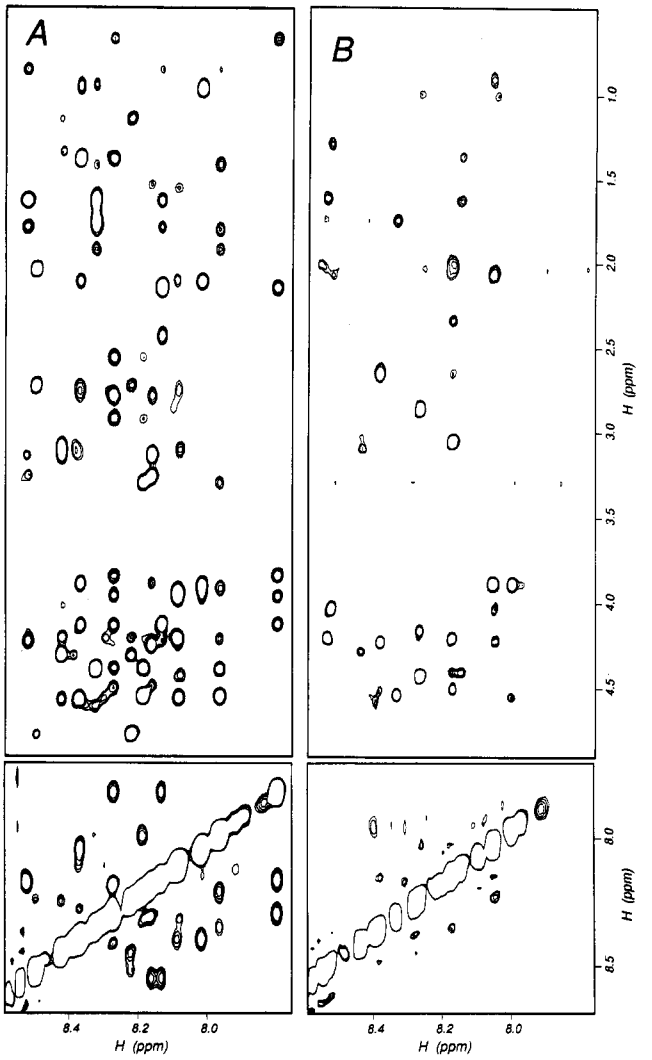

FIGURE 5: Comparison between the 2D NOESY spectra (acquired with a 300-ms mixing time) for peptide 5–21 in (A) 15% TFE and (B) water. The upper section shows the NH to C$^\alpha$H and side chain proton contacts, and the lower section shows the NH–NH contacts.

Leu-14, with evidence of small populations of a longer helix from Thr-6 to Glu-15.

DISCUSSION

Direct NMR Studies Combined with Quantitative Titration. The combination of studying the structure of a family of peptides as a function of [TFE] directly by NMR and indirectly by CD using the equation of Jasanoff and Fersht (1994) has provided some novel insights. A simple ^1H NMR analysis of NOEs shows that, whereas the wild-type peptide in 35% TFE is α-helical in the same sequence as in native barnase (residues 6–18), a destabilizing mutation at position 17 (Tyr→Ala) causes the helix to become truncated in the peptide, extending definitely only from residues 9 to 14 with evidence for some structure from 6 to 15. The quantitative analysis by CD titration provides three parameters from eq 1 that can be used, in general, in conjunction with this information: ΔG^{H_2O}, the free energy of formation of the helix in water; m, the sensitivity of the free energy of formation of the helix to [TFE]/[H_2O]; and $\Delta\Theta_{222}$, the change in the characteristic CD signal for helix formation. In addition, the pK_a of His-18, which is specific to this family, provides important ancillary information.

(i) Effects of Mutation on the pK_a of His-18. The pK_a of His-18 in barnase is raised by two general factors: the

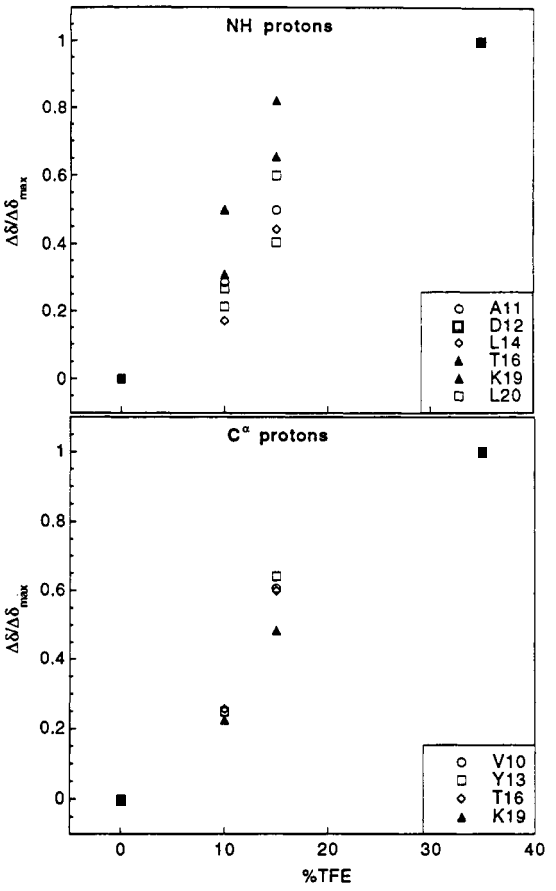

FIGURE 6: Plots of the changes in chemical shift for NH and C^{α} protons against [TFE] for the residues in peptide 5–21 that undergo the largest changes. The changes are normalized, taking the values to be 0 in water and 1.0 in 35% TFE.

interaction of the positively charged imidazolium side chain with the macroscopic dipole of the helix [possibly dominated by the microscopic dipole of the >C=O of Gln-15 with which the imidazole/imidazolium group forms a hydrogen bond (Mauguen et al., 1982; Bycroft et al., 1990)] and the advantage of forming an intramolecular hydrogen bond with Gln-15 in the conformationally restricted helix, rather than an intermolecular hydrogen bond with solvent (Sali et al., 1987; Loewenthal et al., 1991; Sancho et al., 1992a). There is a third and large contribution in wild-type barnase from a histidine–aromatic interaction with Trp-94, so that we use the mutant barnase with Trp-94→Leu as the reference (Loewenthal et al., 1992). The pK_a of His-18 is 7.13 ± 0.01 in the native state of this mutant whereas it is 6.52 ± 0.03 in denatured barnase. It is seen in Table 2 that the pH dependence fits to a pK_a of 6.54–6.56 in the unfolded states (coil) of all of the peptides, but is raised to 7.34 and 7.42 in the α-helical forms of the wild-type peptides 1–22 and 5–21, respectively. The pK_a drops with mutations that cause the helix to be truncated at its C-terminus. Thus, the titration procedure detects the disruption of the C-terminus of the helix since it destroys the helix–dipole–histidinium interaction. Concomitantly, protonation of His-18 at low pH does not stabilize the formation of the mutant helices as much as it does wild-type peptides. There are two possible reasons why the helix–dipole–histidinium interaction is slightly larger in the peptides than in barnase. First, there is likely to be better solvation of the histidinium ion in the peptide. Second, there could be different long range electrostatic effects in the full protein.

(ii) Effects of Mutation on m. The value of m for related peptides previously was found to increase with increasing length, possibly linearly (Jasanoff & Fersht, 1994). The mean value of m for the wild-type peptide is 38 ± 3, whereas it is lowered to 30 ± 4 for the Tyr-17→Ala mutation, consistent with the mutation truncating the helix (Table 1). The value of m is lowered in all of the other mutants, especially in the double Tyr→Ala mutant (= 24 ± 2). This mutant also has a value for the pK_a of His-18 of only 6.7 (Table 2). Thus, inspection of m also detects that mutation truncates the helix.

(iii) Effects of Mutation on ΔG^{H_2O}. Interestingly, the equilibrium constant for the formation of helix in the region that does become helical is not greatly affected by mutation (Table 1). The primary effect of the destabilizing mutations thus is to shorten the helix rather than alter the equilibrium constant.

(iv) Effects of Mutation on $\Delta\Theta_{222}$. Chakrabartty et al. (1993) have pointed out that the presence of Tyr in helices can partially neutralize the CD signal at 222 nm. The spectra here confirm this. $\Delta\Theta_{222}$ is lowered by destabilizing mutations as a result of decreased helix formation in the peptide.

It is common practice to analyze the helix-forming propensities of amino acids from their effects on the percentage of helicity observed by CD. Helix-weakening effects of mutations act here primarily by shortening the length of the helix, with smaller effects on the equilibrium constants between helix and coil. Such effects would not be detected by simple measurements on the percent helicity of peptides measured by the amplitudes of the CD signal at 222 nm, so that the interpretation of such procedures is dangerous in the absence of quantitative titration and/or NMR studies.

Cooperative Induction of Helices by TFE and the Importance of m. The existence of an isodichroic point and the parallel changes of many of the chemical shifts in NMR spectra at concentrations of TFE spanning the transition region (cf. Shin et al., 1993b) show that there is predominantly one major helix being induced by TFE. This is predicted by eq 1 if the value of m increases with length. Suppose there is a mixture of peptides of varying lengths. Then each responds to [TFE] by eq 1, so that each obeys the law

$$K_i^{TFE} = K_i^{H_2O} \exp((m_i/RT)[TFE]/[H_2O]) \qquad (4)$$

If m_i increases with increasing length, as evidence suggests, then the longer helices are favored exponentially with increasing [TFE] because of the weighting factor, $\exp((m_i/RT)[TFE]/[H_2O])$.

There are two consequences of this that must be considered in any analysis. (i) TFE titrations and the direct study of peptides in the presence of [TFE] tend to select the longest helices. The extrapolation of data from high [TFE] to water should give accurate information on the single longest helix, unless there is a mixture of states in the range of [TFE] that is being investigated. (ii) At low concentrations of TFE, shorter helices could predominate. There is some evidence that this may be happening with the wild-type peptide. The deviations in chemical shifts from the random coil values listed in Table 3 appear larger than expected for a very small population of structured states. The acid-unfolded state of barnase has now been completely assigned using heteronuclear NMR methods (Arcus et al., 1994), and similar nonrandom deviations are found for the region 5–18.

Equation 1 is empirical, but it does have a theoretical basis (Jasanoff & Fersht, 1994). The self-consistency of the data obtained upon applying the equation to a related family of peptides and the consistency with direct NMR data suggest

that it should be a useful general tool for probing helical propensity in weakly structured peptides. The combination of CD methods with NMR is exceedingly powerful.

REFERENCES

Arcus, V. L., Vuilleumier, S., Freund, S. V., Bycroft, M., & Lersht, A. R. (1994) *Proc. Natl. Acad. Sci. U.S.A.* (in press).

Bax, A., & Davis, D. G. (1985) *J. Magn. Reson. 65*, 355–360.

Bierzynski, A., Kim, P. S., & Balwin, R. L. (1982) *Proc. Natl. Acad. Sci. U.S.A.* 79, 2470–2474.

Bradford, M. (1976) *Anal. Biochem. 72*, 248–253.

Brems, D. N., Plaisted, S. M., Kauffman, E. W., Lund, M., & Lehrman, S. R. (1987) *Biochemistry 26*, 7774–7778.

Bycroft, M., Sheppard, R. N., Lau, F. T.-K., & Fersht, A. R. (1990) *Biochemistry 29*, 7425–7432.

Chakrabartty, A., Kortemme, T., Padmanabhan, S., & Baldwin, R. L. (1993) *Biochemistry 32*, 5560–5565.

Chen, C. J. H., & Sonnenberg, M. (1977) *Biochemistry 16*, 2110–2118.

Dill, K. A., & Shortle, D. (1991) *Annu. Rev. Biochem. 60*, 795–825.

Dyson, H. J., & Wright, P. E. (1991) *Annu. Rev. Biophys. Biophys. Chem. 20*, 519–538.

Dyson, H. J., Rance, M., Houghten, R. A., Wright, P. E., & Lerner, R. A. (1988) *J. Mol. Biol. 201*, 201–217.

Dyson, H. J., Merutka, G., Waltho, J. P., Lerner, R. A., & Wright, P. E. (1992a) *J. Mol. Biol. 226*, 795–817.

Dyson, H. J., Sayre, J. R., Merutka, G., Shin, H.-C., Lerner, R. A., & Wright, P. E. (1992v) *J. Mol. Biol. 226*, 819–835.

Fersht, A. R. (1985) *Enzyme Structure and Mechanism*, 2nd ed., W.H. Freeman & Co., New York).

Gans, P. J., Lyu, P. C., Manning, M. C., Woody, R. W., & Kallenbach, N. R. (1991) *Biopolymers 31*, 1605–1614.

Gill, S. C., & von Hippel, P. H. (1989) *Anal. Biochem. 182*, 319–326.

Goodman, M., Naider, F., & Toniolo, C. (1971) *Biopolymers 10*, 1719–1730.

Gooley, P. R., & MacKenzie, N. E. (1988) *Biochemistry 27*, 4032–4040.

Jasanoff, A., & Fersht, A. R. (1994) *Biochemistry 33*, 2129–2135.

Jenner, J., Meier, B. H., Bachmann, P., & Ernst, R. R. (1979) *J. Chem. Phys. 71*, 4546–4553.

Karplus, M., Snyder, G. H., & Sykes, B. D. (1973) *Biochemistry 12*, 1323–1329.

Kim, P. S., & Baldwin, R. L. (1990) *Annu. Rev. Biochem. 59*, 631–660.

Kim, P. S., Bierzynski, A., & Baldwin, R. L. (1982) *J. Mol. Biol. 162*, 187–199.

Kippen, A. D., Sancho, J., & Fersht, A. R. (1994) *Biochemistry 33*, 3778–3786.

Kumar, A., Ernst, R. R., & Wüthrich, K. (1980) *Biochem. Biophys. Res. Commun. 95*, 1–5.

Kuroda, Y. (1993) *Biochemistry 32*, 1219–1224.

Lehrman, S. R., Tuls, J. L., & Lund, M. (1990) *Biochemistry 29*, 5590–5596.

Liu, Z. P., Rizo, J., & Gierasch, L. M. (1994) *Biochemistry 33*, 134–142.

Loewenthal, R., Sancho, J., & Fersht, A. R. (1991) *Biochemistry 30*, 6775–6779.

Loewenthal, R., Sancho, J., & Fersht, A. R. (1992) *J. Mol. Biol. 224*, 759–770.

Marion, D., & Wuthrich, K. (1983) *Biochem. Biophys. Res. Commun. 113*, 967–974.

Matouschek, A., & Fersht, A. R. (1993) *Proc. Natl. Acad. Sci. U.S.A. 90*, 7814–7818.

Matouschek, A., Kellis, J. T., Jr., Serrano, L., Byeroft, M., & Fersht, A. R. (1990) *Nature 346*, 440–445.

Matouschek, A., Serrano, L., & Fersht, A. R. (1992) *J. Mol. Biol. 224*, 819–835.

Mauguen, Y., Hartley, R. W., Dodson, E. J., Dodson, G. G., Bricogne, G., Chothia, C., & Jack, A. (1982) *Nature 29*, 162–164.

Merutka, G., & Stellwagen, E. (1989) *Biochemistry 28*, 352–357.

Merutka, G. & Stellwagen, E. (1991) *Biochemistry 30*, 1591–1594.

Merutka, G., Shalongo, W., & Stellwagen, E. (1991) *Biochemistry 30*, 4245–4248.

Moult, J., & Unger, R. (1991) *Biochemistry 30*, 3816–3824.

Nelson, J. W., & Kallenbach, N. R. (1986) *Proteins: Struct. Funct., Genet. 1*, 211–217.

Nelson, J. W., & Kallenbach, N. R. (1989) *Biochemistry 28*, 5256–5261.

Neri, D., Billeter, M., Wider, G., & Wüthrich, K. (1992) *Science 257*, 1559–1563.

Piantini, U., Sorensen, O. W., & Ernst, R. R. (1982) *J. Am. Chem .Soc. 104*, 6800–6801.

Ptitsyn, O. B. (1991) *FEBS Lett. 285*, 176–181.

Redfield, A. G., & Kunz, S. D. (1975) *J. Magn. Reson. 19*, 250–254.

Sali, D., Bycroft, M., & Fersht, A. R. (1988) *Nature 335*, 740–743.

Sancho, J., & Fersht, A. R. (1992) *J. Mol. Biol. 224*, 741–747.

Sancho, J., Serrano, L., & Fersht, A. R. (1992a) *Biochemistry 31*, 2253–2258.

Sancho, J., Neira, J. L., & Fersht, A. R. (1992b) *J. Mol. Biol. 224*, 749–758.

Scholtz, J. M., Qian, H., York, E. J., Stewart, J. M., & Baldwin, R. L. (1991) *Biopolymers 31*, 1463–1470.

Serrano, L., Kellis, J. T., Jr., Cann, P., Matouschek, A., & Fersht, A. R. (1992) *J. Mol. Biol. 224*, 783–804.

Shin, H.-C., Merutka, G., Waltho, J. P., Wright, P. E., & Dyson, H. J. (1993a) *Biochemistry 32*, 6348–6355.

Shin, H.-C., Merutka, G., Waltho, J. P., Tennant, L. L., Dyson, H. J., & Wright, P. E. (1993a) *Biochemistry 32*, 6356–6364.

Shoemaker, K. R., Kim, P. S., Brems, D. N., Marqusee, S., York, E. J., Chaiken, I. M., Stewart, J. M., & Baldwin, R. L. (1985) *Proc. Natl. Acad. Sci. U.S.A. 82*, 2349–2353.

Shortle, D., & Meeker, A. K. (1986) *Proteins: Struct., Funct., Genet. 1*, 81–89.

Shortle, D., & Meeker, A. K. (1989) *Biochemistry 28*, 936–944.

Sönnichsen, F. D., Van Eyk, J. E., Hodges, R. S., & Sykes, B. D. (1992) *Biochemistry 32*, 8790–8798.

Tanford, C. (1968) *Adv. Protein Chem. 23*, 121–282.

Tanford, C. (1970) *Adv. Protein Chem. 24*, 1–95.

Vuilleumier, S., Sancho, J., Loewenthal, R., & Fersht, A. R. (1993) *Biochemistry 32*, 10303–10313.

Waltho, J. P., Feher, V. A., Merutka, G., Dyson, H. J., & Wright, P. E. (1993) *Biochemistry 32*, 6337–6347.

Wishart, D. S., Sykes, B. D., & Richards, F. M. (1991) *J. Mol. Biol. 222*, 311–333.

Woody, R. W. (1985) *Peptides 7*, 15–114.

Wright, P. E., Dyson, H. J., & Lerner, R. A. (1988) *Biochemistry 27*, 7167–7175.

Wüthrich, K. (1986) *NMR of Proteins and Nucleic Acids*, John Wiley and Sons, New York.

Yoshida, K., Shibata, T., Masai, J., Sato, K., Noguti, T., Go, M., & Yanagawa, H. (1993) *Biochemistry 32*, 2162–2166.